NASA Technical Memorandum 105558

Design Feasibility Study of a Space Station Freedom Truss

Sasan C. Armand
Lewis Research Center
Cleveland, Ohio

and

Caroline A. Dohogne
University of Michigan
Ann Arbor, Michigan

April 1992

NASA

DESIGN FEASIBILITY STUDY OF SPACE STATION (SHORT) SPACER TRUSS

Sasan C. Armand and Caroline A. Dohogne
National Aeronautics and Space Administration
Lewis Research Center
Cleveland, Ohio 44135

SUMMARY

The study presented in this paper focuses on the design and configuration feasibility of the short spacer for the Space Station Program in its launch configuration. The product of this study is being used by Rockwell International (Rocketdyne Division) as they continue their design concept of the current short spacer configuration. It is anticipated that the launch loads will dominate the on-orbit loads and dictate the design configuration of the short spacer. At the present time the on-orbit loads have not been generated. The structural analysis discussed herein is based on the transient events derived from the Space Transportation System (STS) Interface Control Document (ICD). The transient loading events consist of liftoff loads, landing loads, and emergency landing loads. The quasi-static loading events have been neglected, since the magnitude of the acceleration factors are lower than the transient acceleration factors. The normal mode analyses presented herein are based on the most feasible configurations with acceptable stress ranges.

INTRODUCTION

Space Station Freedom (fig. 1(a)) is a low-Earth-orbit (220 nmi) manned spacecraft that is currently being designed and developed by NASA, Japan, Europe, and Canada. NASA Lewis Research Center is responsible for developing the two solar power modules (three photovoltaic power module). Each module consists of photovoltaic solar array assemblies, beta gimbal assemblies, integrated equip-ment assembly (IEA), a thermal control subsystem, and spacer trusses (long and short). The short spacer truss is the focus of this paper.

It will take 17 shuttle flights to assemble Space Station Freedom. The three photovoltaic power modules will be launched on the first, tenth, and fourteenth flights. Figure 1(b) shows the solar power module consisting of two photovoltaic power modules. The photovoltaic power modules carried on the tenth (inboard) and the fourteenth (outboard) shuttle flights are connected through a rectangular cross section truss. The assembled distance between the inboard and outboard photovoltaic power modules is 590 in., which corresponds to the distance (minimum) where the effect of shadowing from the inboard/ outboard solar array on the outboard/inboard solar array is minimized. Since the maximum length of any cargo element in the STS cargo bay is 540 in., the 590-in. outboard photovoltaic module cargo element must be split into two cargo elements; namely, the photovoltaic power module integrated with a long spacer and the short spacer (fig. 2). The eleventh STS launch will carry the short spacer.

FINITE-ELEMENT ANALYSIS

This section describes the finite-element model generated for the structural and normal mode analyses.

Overall Modeling Strategy

The finite-element model generated for the structural and normal mode analyses is a three-dimensional model of the short spacer which contain 852 degrees of freedom (fig. 3). The finite-element model primarily contains linear isoparametric beam elements (known per ref. 1 as BAR elements). The BAR element is a two–noded beam element with a capability of predicting axial, bending, and torsional stresses. Concentrated mass elements have also been used to account for some of the nonstructural masses such as mobile transporter rails with their support structure and truss interconnects. To account for the mass of the components whose locations and exact magnitudes have not yet been determined, an uncertainty factor of 1.5 was applied to the loads from the STS ICD.

The material (Inconel 718) and the sizes of the longeron trunnions (3.244-in. diameter) and the keel trunnion (2.996-in. diameter) are discussed in reference 2. The trunnions were all modeled using the BAR elements, and the weight and the mass moment of inertia of the scuff plates were modeled as concentrated mass elements with proper offset of their centers of gravity from their supporting nodes.

The material (aluminum 6061-T6) and the sizes of the tubes for the longerons, battens, and diagonals were chosen to be the same. Although two sizes of tubes in the overall analysis were chosen - namely, a 3.0-in. outer diameter tube and a 2.5-in. outer diameter tube - the wall thickness selected for both sizes was 0.2 in.

Failure Criteria

The failure criteria considered in this study are based on the stresses and displacements (deformation) obtained from the structural computer runs and the circular frequencies obtained from the normal mode computer runs and comparing their values to the allowables per references 3 and 2, respectively. The displacements of payloads are of particular concern since the payloads should have enough structural rigidity to stay within the dynamic envelope of the shuttle bay. However, since the drawings of the short spacer cargo element have not yet been developed, the clearances between the short spacer truss and the cargo bay internal envelope are unknown. Thus, the displacement failure criterion was selected to be 1.0 in., which is the same as the displacement of IEA in its launch configuration. The nodes where the displacements are recovered are shown in figure 5. These nodes are the closest points to the cargo bay and should have the maximum displacements, as was verified later on.

The circular frequencies obtained from the normal mode computer runs were compared to minimum allowable frequencies (ref. 2). For the combined weight category of the short spacer cargo element and the starboard node cargo element (30,000 lb), the minimum frequency is 6.0 Hz. Not meeting the minimum frequency does not necessarily mean that the cargo element will fail, but it is a flag for NASA to start preparing for a control-structure interaction study. This study is primarily done to analyze the interaction of the payload with the control of the space shuttle during flight. If a payload does not meet the frequency requirement and does not interact with the control of the shuttle, the design may be acceptable. To avoid a control-structure interaction study at this early stage of the design work, it was decided to consider the minimum frequency requirement as a failure criteria.

One more failure criteria which would have been appropriate to check for was the buckling of the short spacer under the launch loads. However, since all the member sizes are the same, it was determined that any possible local buckling can easily be avoided by adding local stiffeners and that any system buckling can be avoided by adding battens and/or diagonals. Therefore, no buckling analysis was performed for this feasibility study.

In conclusion, sizing the structural members and locating masses on the short spacer were based first on meeting the allowable strength and second on any deformation at any of the eight corners of the structure. The structural models that met the allowable strength and had the lowest weight were then analyzed for the circular frequencies.

Test Criteria

Reference 4 offers three options for a static test. The strength margins of safety calculated in this study are influenced by the option selected. NASA Lewis uses the second option of this requirement which is as follows:

> . . .static test the payload to 1.2 times the design limit load. This test shall verify the static analytical math model such that the design can be verified for ultimate load capability by a detailed and formal stress analysis. The ultimate design factor of safety for the analysis shall be 1.4 or greater.

The requirements in reference 4 were designed to ensure that no damage will result to STS, regardless of whether the payload can function or not after launch to orbit. Since the truss spacers have functions (i.e., support the mobile transporter rail which may have small tolerances) and no yielding should be allowed, an additional factor of safety of 1.1 is used on the yield strength of the material to eliminate the possibility of any yielding. Therefore, the margin of safety will be calculated based on the lower of the values determined by dividing the ultimate strength of the material by 1.4 and by dividing the yield strength of the material by 1.1.

Structural Analysis

The mechanism of loading in the shuttle bay during launch is through the gravitational accelerations in the six directions imposed on the structure. The acceleration loads used in this analysis (obtained from ref. 5) are shown in table I. The table shows that loads vary from a negative value to a positive value in all directions. Therefore, all the loads in all six directions had to be combined in all possible combinations to ensure that the maximum stresses and displacements could be determined. The total number of load cases for each structural computer run turned out to be 136.

Normal Mode Analysis

The dynamic models used for the normal mode analysis were converted structural models.

One of the modeling checks done on the finite-element dynamic model prior to the normal mode and dynamic analyses is recovering and checking the rigid body modes to ensure that there is no artificial grounding in the finite-element model. The finite-element models of the short spacer truss were freed at the trunnions, and, as it turned out, there were six distinct rigid body modes with near zero frequencies in six directions - three translations and three rotations.

RESULTS

In performing the structural analysis of the short spacer truss two configurations of the structure were analyzed - namely, the loaded configuration and the off-loaded configuration. In the off-loaded configuration the MT/CETA rails and their mounting structures are off-loaded from the launch element. With each configuration two different tube sizes were used - namely a 3.0-in. outer diameter tube and a

2.5-in. outer diameter tube. The structural analysis of the loaded configuration indicated that, regardless of member size and stiffeners, the stresses are always beyond and above the allowable stress of 30 000 psi; thus, without a major configuration change an acceptable design cannot be achieved. Therefore, in this paper only the results for the off-loaded spacer truss have been reported. The early structural analysis of the short spacer indicated that the maximum stress always occurs at the joint between the batten beam and the scuff plate and its magnitude is not so much a function of the tube size but is, in reality, a function of the stiffness of the batten beam. Thus, the moment of inertia of the cross section of the batten beam was increased by making the beam solid. Table II shows the description of all structural computer runs made. The computer runs shown in table III, rows 3 and 4, are representative of structural models with solid batten beams. One typical stress plot of the short spacer with hollow batten beams is shown in figure 6. Note that the maximum stress always occurs in the batten beam (aluminum section) interfaces as expected. In this figure, four views of the short spacer truss have been shown. Note that this stress plot is from the SDRC post-processing code which uses an averaging scheme and the stress contour pallet on the right side of each figure does not represent the true maximum stresses.

The last improvement made to the structural model was to make sections of the batten beams extending from the shuttle restraining points to the 5-point joints from solid Inconel. This was done since these areas were highly stressed, and the weight increase of using solid Inconel was relatively minimal. The stresses reported in table III, rows 5 and 6, are representative of the last improvement to the structural model. The stress contour plots for rows 4 to 6 of table III are shown in figures 7 to 9.

The displacements from the structural computer runs (table III, rows 1 to 6) were recovered, and the maximum resultant values in three translational directions are reported in table IV. The displacement for all computer runs indicated satisfactory results based on the 1.0 in. displacement criteria. The displacement plots for rows 4 to 6 of table IV are shown in figures 10 to 12.

Since all the short spacer configurations (table III) have acceptable stresses and displacements, the same configurations were used for normal mode analysis. The fundamental frequencies for the short spacer with 2.5- and 3.0-in. aluminum tubes are all above the minimum frequency requirement of 6.0 Hz. The mode shape plots for all configurations of the short spacer are similar, and they are shown in figures 13 to 16. The frequency values are tabulated in table V. Examining these plots, for the first modes, shows some level of bending activity around the keel and the longeron trunnions. This particular mode can be categorized as a system mode, since the entire structure is vibrating. Modes 2 to 5 can be categorized as local modes, and mode 6 can again be categorized as a system mode.

CONCLUSION

The structural analysis indicates that the most feasible tube size for the short spacer is a 3.0-in. outer diameter. The weight difference between a short spacer with a 3.0-in. outer diameter tube and the one with a 2.5-in. outer diameter tube is approximately 110 lb; however, using a 3.0-in. outer diameter tube reduces the stress levels by approximately 5000 psi. There is a slight advantage to making the batten beams of solid aluminum or solid Inconel; the stress levels drop by a small percentage, and the fundamental circular frequency increases by approximately 3.0 Hz. Any decrease in stress levels and/or increase in fundamental circular frequency will provide the opportunity to accommodate increases in nonstructural mass without a major design change in the future. The maximum displacement under the worst loading condition turned out to be 0.399 in., which can be looked upon as an acceptable displacement.

REFERENCES

1. Joseph, J.A.: MSC/NASTRAN Application Manual. The MacNeal-Schwendler Corp., 1984.

2. National Space Transportation System. NSTS 20052, Vol. 8, Structural/Mechanical Interfaces and Requirements. NASA Johnson Space Center, 1988.

3. Military handbook. Metallic Materials and Elements for Aerospace Vehicle Structures. MiL-HDB-5, June 1987.

4. National Space Transportation System. NSTS 14046, Rev. B, Payload Verification Requirements. NASA Johnson Space Center, 1982.

5. National Space Transportation System. NSTS 07700, ICD-2-19001, Rev. K, Shuttle Orbiter/Cargo Standard Interfaces. NASA Johnson Space Center, 1991.

TABLE I.—CARGO LIMIT - LOAD FACTORS/ANGULAR ACCELERATIONS FOR PRELIMINARY DESIGN (TRANSIENT FLIGHT EVENTS)

Flight event	Load factor, g			Acceleration, rad/sec^2			Cargo weight
	N_x	N_y	N_z	$\ddot{\phi}$	$\ddot{\Theta}$	$\ddot{\Psi}$	
Ascent:							
Liftoff	−0.2 −3.2	±1.4	2.5 −2.5	±3.7	±7.7	±3.1	Up to 65 Klb (29 484 kg)
Descent:							
Landing	1.8 −2.0	±1.5	4.2 −1.0	±6.4	±11.3	±4.9	Up to 32 Klb (14 515 kg)
Emergency landing:							
Outside crew	+4.5	+1.50	+4.5				
Compartment	−1.5	−1.50	−2.0				

TABLE II.—DESCRIPTION OF COMPUTER RUNS FOR USE IN TABLES III TO IV AND FIGURE 5

Computer run	Tube diameter, in.	Batten beam	Portion batten beam connecting cross battens to scuff plates
1	2.5	Hollow	Aluminum
2	3.0	Hollow	Aluminum
3	2.5	Solid	Aluminum
4	3.0	Solid	Aluminun
5	2.5	Solid	Inconel
6	3.0	Solid	Inconel

TABLE III.—MODEL WEIGHT, MAXIMUM STRESS AT EACH TRANSIENT EVENT, AND MARGIN OF SAFETY FOR COMPUTER RUNS DESCRIBED IN TABLE II

Computer run[a]	Weight, lb	Liftoff, psi	Landing, psi	Emergency landing, psi	Allow-able, psi	Margin of saftey
1	749	16 589	[b]22 596	16 688	30 000	0.33
2	858	12 814	[b]17 258	12 801	↓	.74
3	772	11 072	[b]16 013	11 807		.87
4	893	9 563	[b]14 615	10 778		1.05
5	837	15 852	[b]24 068	17 662		.25
6	987	11 115	[b]16 931	12 457		.77

[a]See table I for description of computer runs.
[b]Maximum stress among three transient events.

TABLE IV.—MAXIMUM DISPLACEMENTS FOR NODES SHOWN IN FIGURE 5 AND COMPUTER RUNS DESCRIBED IN TABLE II

Computer run[a]	Node	Load event	Displacement
1	47	Landing	0.399
2	↓	↓	.283
3			.332
4			.234
5			.253
6			.193

[a]See table I for description of computer runs.

TABLE V.—FIRST SIX FREQUENCIES OF THE SHORT SPACER FOR COMPUTER RUNS DESCRIBED IN TABLE II

Computer run[a]	Mode 1, Hz	Mode 2, Hz	Mode 3, Hz	Mode 4, Hz	Mode 5, Hz	Mode 6, Hz
1	14.47	16.72	16.91	17.88	18.72	21.76
2	17.38	20.13	20.32	21.71	22.79	26.14
3	18.11	20.34	20.82	21.76	23.00	26.48
4	15.08	16.92	17.20	17.91	18.91	23.26
5	15.75	16.93	17.58	17.93	19.21	23.70
6	18.63	20.33	21.24	21.80	23.10	26.34

[a]See table I for description of computer runs.

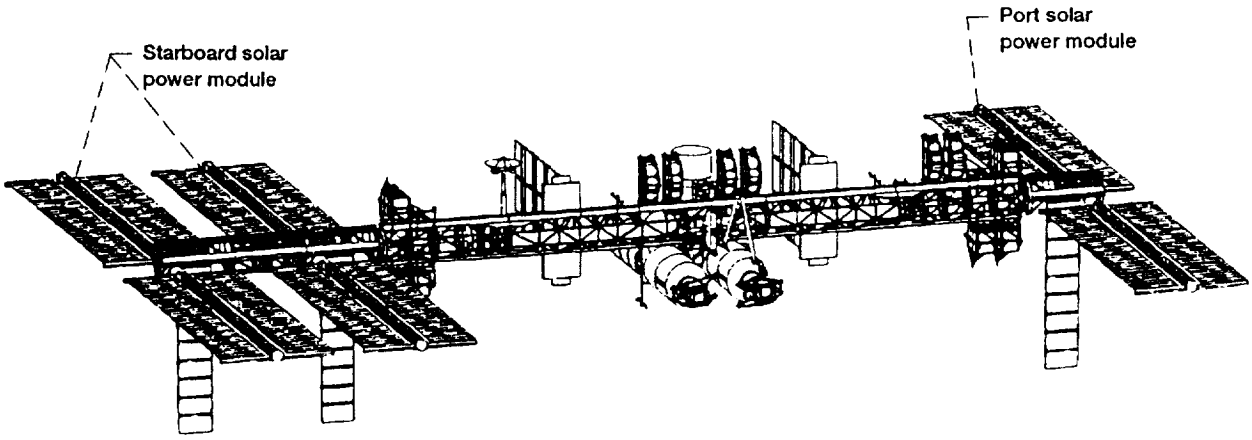

(a) Permanently manned capability.

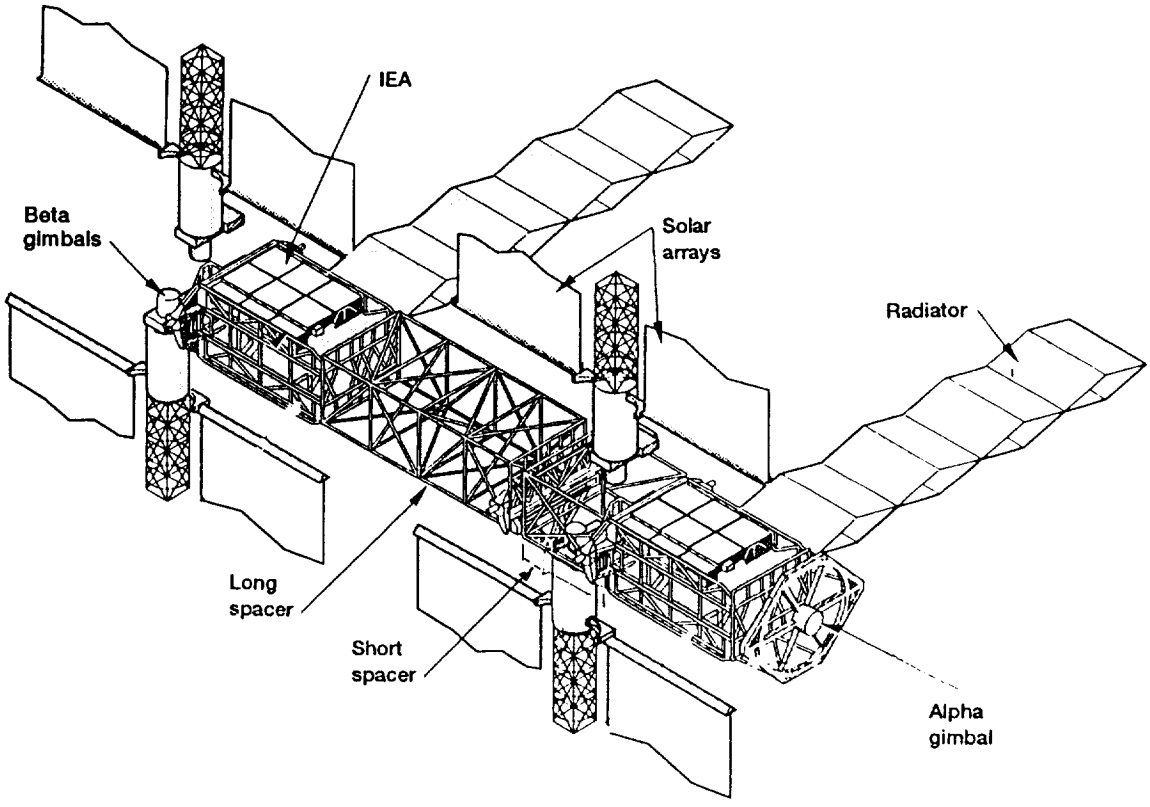

(b) Configuration outboard of alpha gimbal.

Figure 1.— Space Station Freedom.

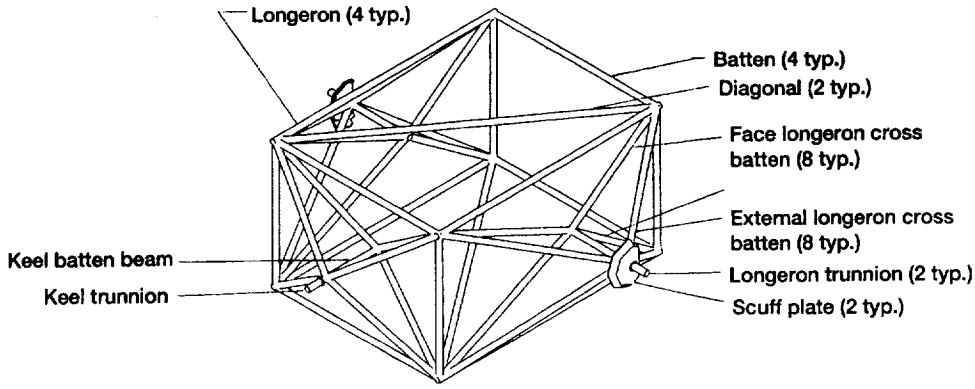

Figure 2.—Short spacer truss.

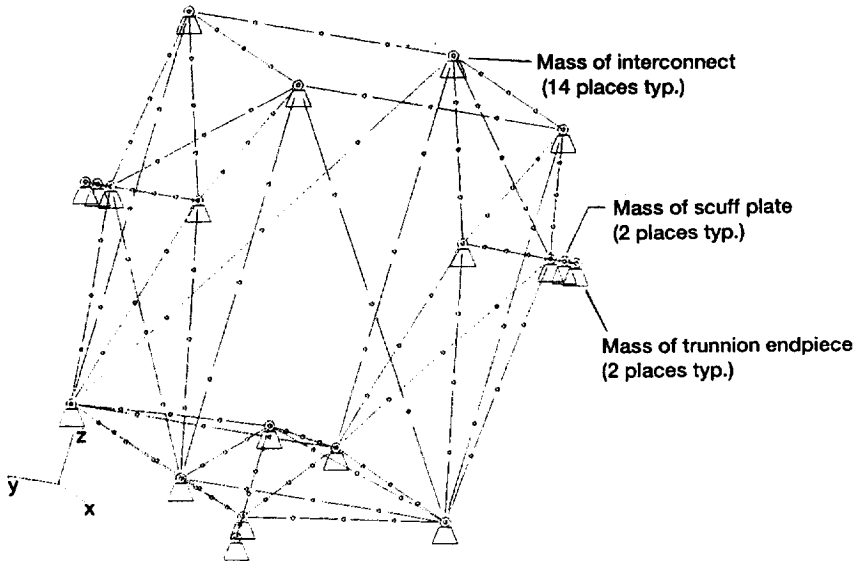

Figure 3.—Structural/dynamic model of short spacer truss.

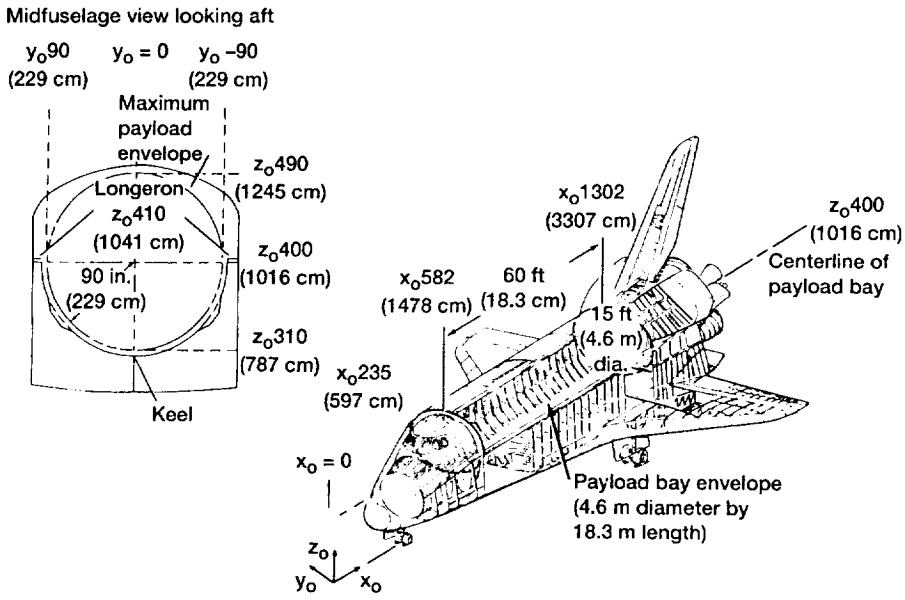

Figure 4.—Description of space transportation system axes.

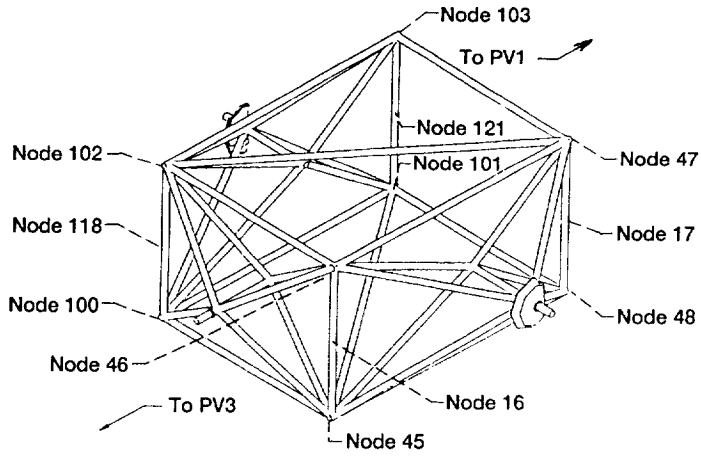

Figure 5.—Node map for displacement recovery.

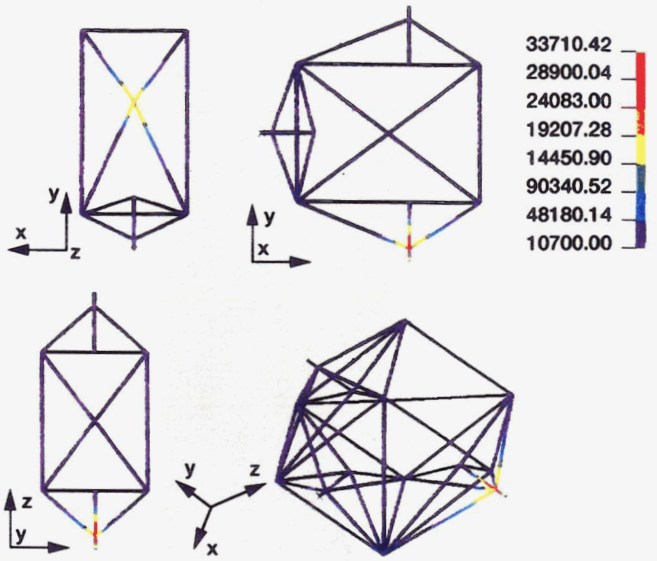

Figure 6.—Typical stress plot for short spacer structure with hollow batten beams.

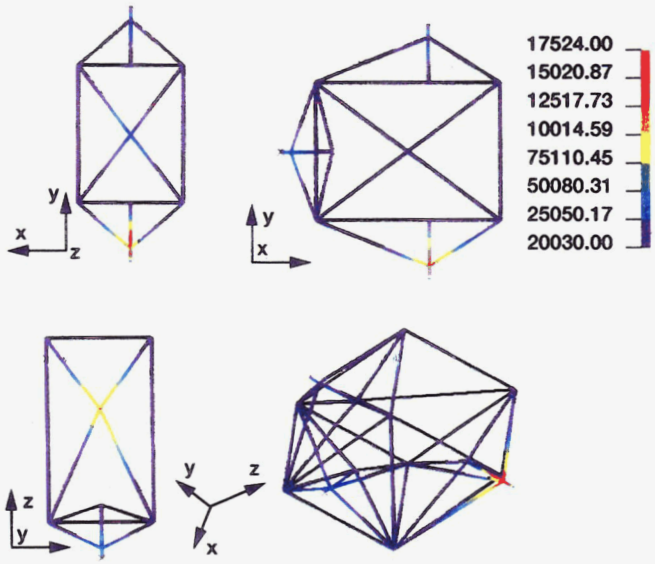

Figure 7.—Stress plot for short computer run 3 (see table III).

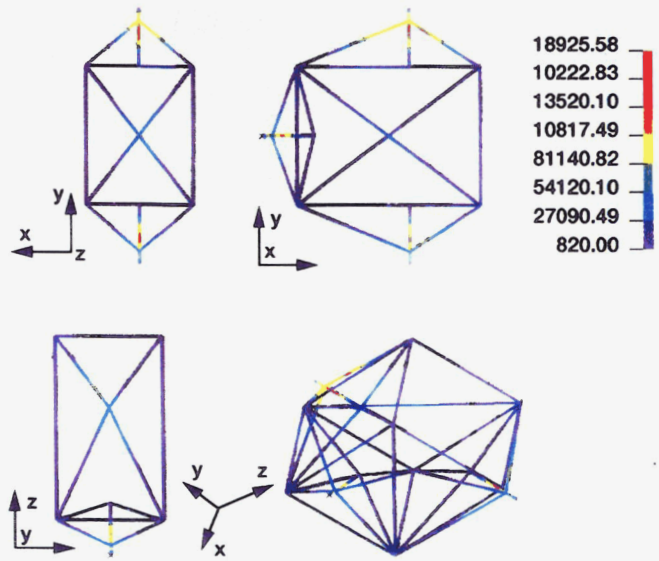

Figure 8.—Stress plot for short computer run 3 (see table III).

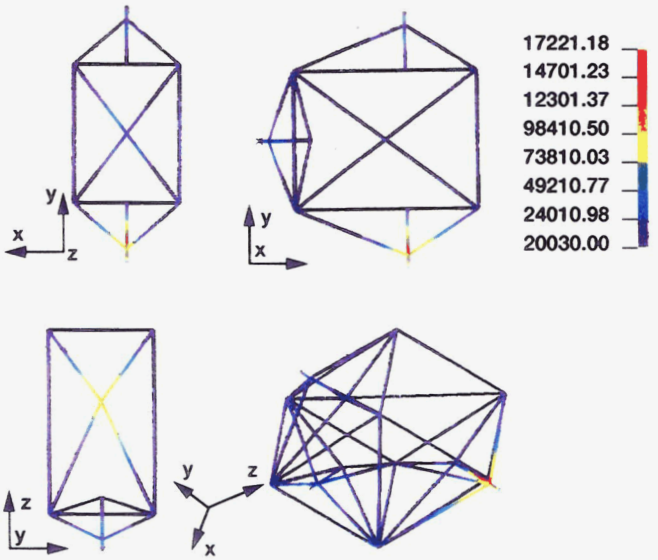

Figure 9.—Stress plot for short computer run 6 (see table III).

ORIGINAL PAGE
COLOR PHOTOGRAPH

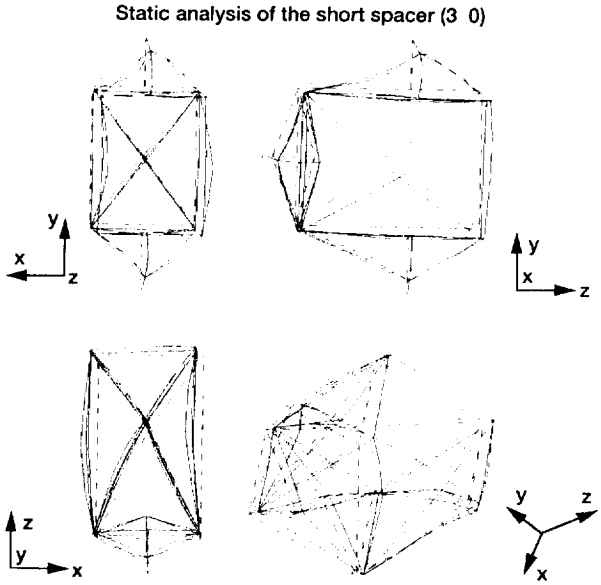

Figure 10.—Displacement plot for computer run 3 (see table IV).

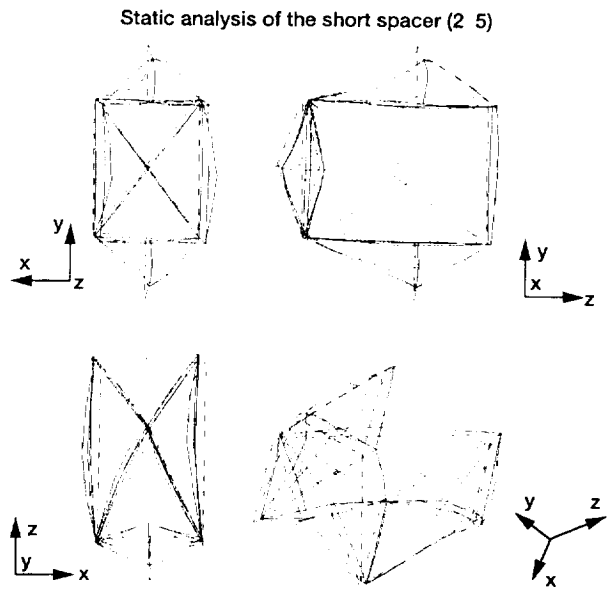

Figure 11.—Displacement plot for computer run 5 (see table IV).

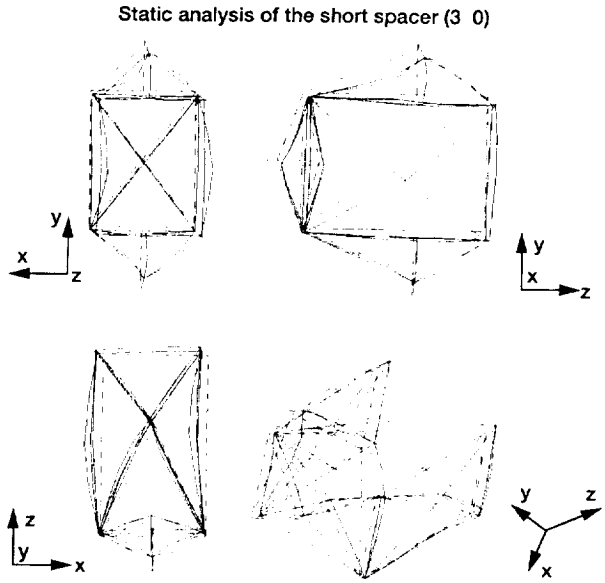

Figure 12.—Displacement plot for computer run 6 (see table IV).

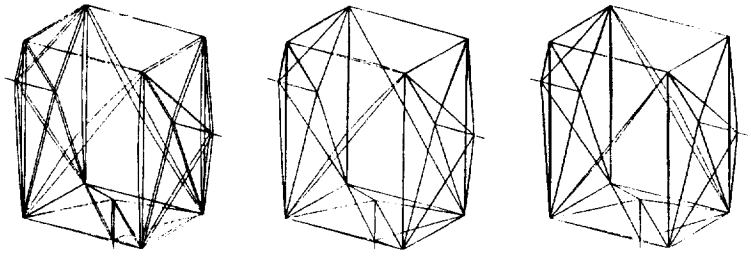

Mode 1 Mode 2 Mode 3

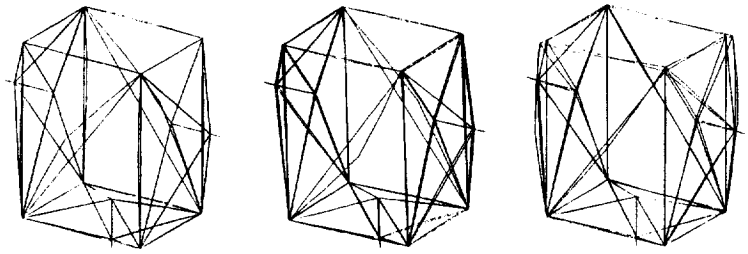

Mode 4 Mode 5 Mode 6

Figure 13.—Mode shapes of short spacer, orthogonal view.

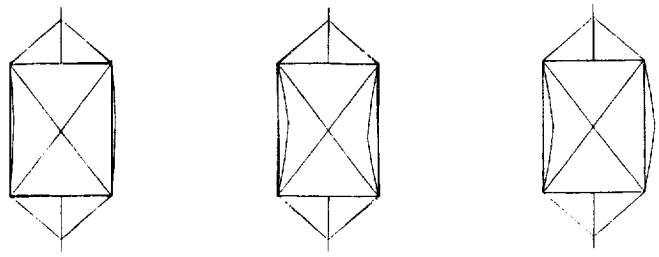

Mode 1 Mode 2 Mode 3

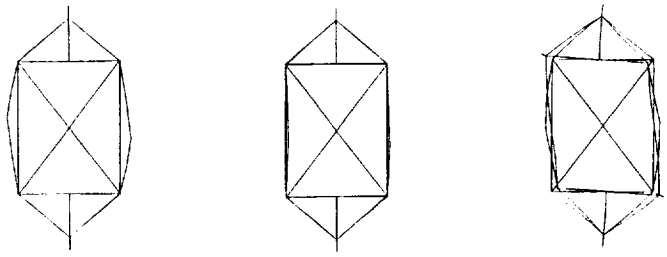

Mode 4 Mode 5 Mode 6

Figure 14.—Mode shapes of short spacer, top view.

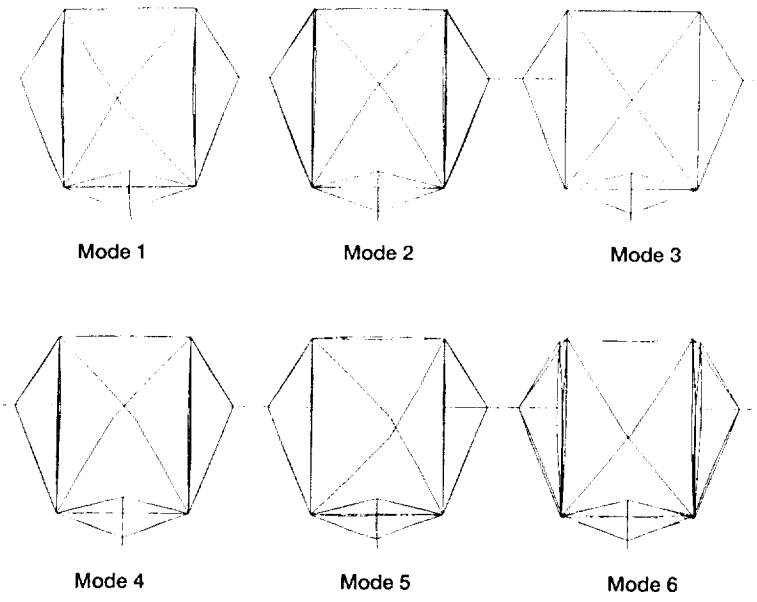

Figure 15.—Mode shapes of short spacer, plan view.

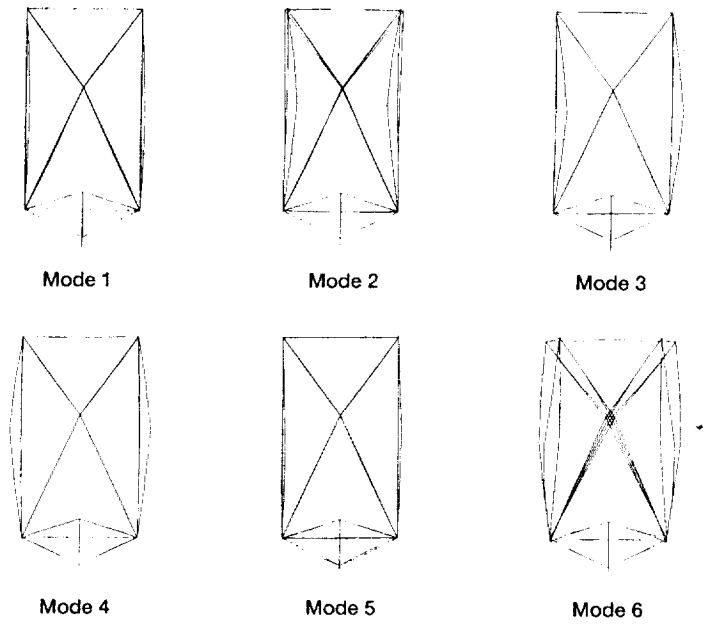

Figure 16.—Mode shapes of short spacer, side view.

REPORT DOCUMENTATION PAGE

Form Approved
OMB No. 0704-0188

1. AGENCY USE ONLY (*Leave blank*)	2. REPORT DATE	3. REPORT TYPE AND DATES COVERED
	April 1992	Technical Memorandum

4. TITLE AND SUBTITLE
Design Feasibility Study of a Space Station Freedom Truss

5. FUNDING NUMBERS
WU-474-46-10

6. AUTHOR(S)
Sasan C. Armand and Caroline A. Dohogne

7. PERFORMING ORGANIZATION NAME(S) AND ADDRESS(ES)
National Aeronautics and Space Administration
Lewis Research Center
Cleveland, Ohio 44135-3191

8. PERFORMING ORGANIZATION REPORT NUMBER
E-6882

9. SPONSORING/MONITORING AGENCY NAMES(S) AND ADDRESS(ES)
National Aeronautics and Space Administration
Washington, D.C. 20546-0001

10. SPONSORING/MONITORING AGENCY REPORT NUMBER
NASA TM-105558

11. SUPPLEMENTARY NOTES
Sasan C. Armand, NASA Lewis Research Center. Caroline A. Dohogne, University of Michigan, Ann Arbor, Michigan 48109. Responsible person, Sasan C. Armand, (216) 433-6734.

12a. DISTRIBUTION/AVAILABILITY STATEMENT
Unclassified - Unlimited
Subject Categories 37 and 39

12b. DISTRIBUTION CODE

13. ABSTRACT ***(Maximum 200 words)***

The study presented in this paper focuses on the design and configuration feasibility of the short spacer for the Space Station Program in its launch configuration. The product of this study is being used by Rockwell International (Rocketdyne Division) as they continue their design concept of the current short spacer configuration. It is anticipated that the launch loads will dominate the on-orbit loads and dictate the design configuration of the short spacer. At the present time the on-orbit loads have not been generated. The structural analysis discussed herein is based on the transient events derived from the Space Transportation System (STS) Interface Control Document (ICD). The transient loading events consist of liftoff loads, landing loads, and emergency landing loads. The quasi-static loading events have been neglected, since the magnitude of the acceleration factors are lower than the transient acceleration factors. The normal mode analyses presented in this paper are based on the most feasible configurations with acceptable stress ranges.

14. SUBJECT TERMS	15. NUMBER OF PAGES
Linear; Normal mode analyses; Space station truss	16
	16. PRICE CODE: A03

17. SECURITY CLASSIFICATION OF REPORT	18. SECURITY CLASSIFICATION OF THIS PAGE	19. SECURITY CLASSIFICATION OF ABSTRACT	20. LIMITATION OF ABSTRACT
Unclassified	Unclassified	Unclassified	